Myosin I Is Required for Hypha Formation in *Candida albicans*†

U. Oberholzer,[1]* A. Marcil,[1] E. Leberer,[2]‡ D. Y. Thomas,[3,4]§ and M. Whiteway[1,3]

Genetics Division, Biotechnology Research Institute, National Research Council of Canada, Montreal, Quebec H4P 2R2,[1] and Departments of Biology,[3] Anatomy and Cell Biology,[4] and Experimental Medicine,[2] McGill University, Montreal, Quebec H3A 2B2, Canada

The pathogenic yeast *Candida albicans* can undergo a dramatic change in morphology from round yeast cells to long filamentous cells called hyphae. We have cloned the *CaMYO5* gene encoding the only myosin I in *C. albicans*. A strain with a deletion of both copies of *CaMYO5* is viable but cannot form hyphae under all hypha-inducing conditions tested. This mutant exhibits a higher frequency of random budding and a depolarized distribution of cortical actin patches relative to the wild-type strain. We found that polar budding, polarized localization of cortical actin patches, and hypha formation are dependent on a specific phosphorylation site on myosin I, called the "TEDS-rule" site. Mutation of this serine 366 to alanine gives rise to the null mutant phenotype, while a S366D mutation, the product of which mimics a phosphorylated serine, allows hypha formation. However, the S366D mutation still causes a depolarized distribution of cortical actin patches in budding cells, similar to that in the null mutant. The localization of CaMyo5-GFP together with cortical actin patches at the bud and hyphal tips is also dependent on serine 366. Intriguingly, the cortical actin patches in the majority of the hyphae of the mutant expressing *Camyo5^{S366D}* were depolarized, suggesting that although their distribution is dependent on myosin I localization, polarized cortical actin patches may not be required for hypha formation.

Polarized growth is a regulated cellular expansion which underlies many processes, such as phagocytosis in mammalian cells, morphogenesis of root hair and other specialized cell types in plants, cell locomotion in *Acanthamoeba* and *Dictyostelium*, and hypha formation in fungi (19, 24, 37, 49). *Saccharomyces cerevisiae* cells can elongate into pseudohyphae in response to specific environmental cues, and polarization of the actin cytoskeleton is essential for this differentiation (11). Similarly, hyphal morphogenesis in other fungi, such as *Saprolegnia ferax*, *Neurospora crassa*, and *Aspergillus nidulans*, requires filamentous actin, while microtubules play a secondary role (20, 51, 52). The pathogenic yeast *Candida albicans* can undergo a dramatic change in morphogenesis when round yeast cells form highly elongated filaments called hyphae, but little is known about the role of the actin cytoskeleton during hypha formation in this organism (25). Treatment of germinating cells with cytochalasin A prevents further hyphal growth, suggesting that filamentous actin is critical to hyphal growth (2). Nocodazole, in contrast, does not prevent apical cell elongation, suggesting that microtubules are not critical for polarized growth in *C. albicans* (61).

Two forms of actin appear to be important during polarized growth. First, actin cables serve as tracks for the vesicular transport of molecular components of the plasma membrane and cell wall toward the site of growth, i.e., the bud tip (23, 44,

45) and presumably the hyphal tip of *C. albicans*. These run along the longitudinal axis of yeast and hyphal cells in *S. cerevisiae* and *C. albicans* (4, 44). Second, cortical actin patches correlate with sites of targeted secretion and endocytosis, critical during cell wall biogenesis (44). These localize to the tips of emerging buds as well to growing hyphal tips in *C. albicans* (4). Proteins that modulate the structure of the actin cytoskeleton are key factors in determining cell polarity (44). Myosin I, one of these factors, is a single-headed molecular motor that functions in actin-based processes such as polarized growth, cell motility, phagocytosis, endocytosis and exocytosis, and contractile vacuolar activity in several organisms (12, 13, 32, 37, 40, 46, 50, 58). In *S. cerevisiae*, myosin I was shown to promote actin polymerization at cortical patches, which correlate with sites of growth (1, 14, 29). This myosin I regulation of actin polymerization was shown to be achieved by its interaction with and activation of the Arp2/3 complex, which nucleates the assembly of actin filaments (14, 29, 33, 34). Similarly, in *Schizosaccharomyces pombe*, myosin I is required for a polarized actin cytoskeleton and was shown to bind to the Arp2/Arp3 complex and activate its actin nucleation activity (32, 53). Jung et al. (22) also found that *Dictyostelium* myosin I interacts with the Arp2-Arp3 complex via the CARMIL protein and may localize actin polymerization to sites of cellular growth. In accordance with its proposed role in polarized growth, myosin I colocalizes with cortical actin patches at the tips of buds in *S. cerevisiae* and of growing cells in *S. pombe* (3, 32, 53) and localizes as well to the tips of hyphae in *Aspergillus* (36).

The actin-dependent ATPase activity of *Acanthamoeba* myosin I and *Dictyostelium* myosin I is activated by the phosphorylation of a unique site, called the "TEDS-rule" site, by members of the p21-activated kinase (PAK) kinases (7, 9, 56). The corresponding phosphorylation site of *S. cerevisiae* myosin I is essential for its function in vivo and for its ability to polymerize

---

* Corresponding author. Mailing address: Genetics Division, Biotechnology Research Institute, 6100 Royalmount, Montreal, Quebec H4P 2R2, Canada. Phone: (514) 496-6358. Fax: (514) 496-6213. E-mail: ursula.oberholzer@nrc.ca.

‡ Present address: Aventis Genomics Center, Aventis Pharma, Martinsried D-82152, Germany.

§ Present address: Chair of Biochemistry, McGill University, Montreal, Quebec H3G 1Y6, Canada.

TABLE 1. Oligonucleotides

Oligonucleotide	Sequence[a]
UO5	GCGGATCCCTGACCTTACACTGTCGTTGG
UO6	GCTCTAGACATTGGCCCACTTGTGGAGGTTC
UO9	CGGGGTACCCAATACTAGATCCTCTGG
UO10	CGGGGATCCAGACTGCAGCCTCTTTTCACAATAGCC
UO11	CGGGGATCCGAAGAAGAAGACGATGATG
UO19	GCGGATCCATGGCTATTGTGAAAAGAGG
UO20	GCAGATCTCATTGGCCCACTTGTGGAGGTTC
UO26	GCAAGCTTACGCCTGCAGTAGGTAAGAACTTGTTATATTTTG
UO27	CTGCAGGCGTAAGCTTGCCCAATCATCATCGTCTTC
UO28	GGGATGAGACGAGGTGCAACTTATCAT
UO29	GGTGAATGATAAGTTGCACCTCGTCTCATCCC
UO30	GGGATGAGACGAGGTGACACTTATCATTCACC
UO31	GGTGAATGATAAGTGTCACCTCGTCTCATCCC
UO36	CGGGGTACCAAGCTTCCAAAGATTGG
UO37	CGGGGATCCAGAGCGGCCGCCCTCTTTTCACAATAGCC
CB20F	CGGGCGGCCGCGGTACCTACCTGGAGGTGAGGAG
CB20R	CGGGGATCCAATATTTATGAGAAACTATCACTTC
Reverse	GGAAACAGCTATGACCATG

[a] Restriction sites used for cloning are underlined in UO5 to UO27 and UO36 to CB20R. Codons mutated for site-directed mutagenesis are underlined in UO28 and UO29.

actin in vitro (29, 57). It is also a target of the Ste20p and Cla4p kinases in vitro (57). These latter proteins are members of the PAK family of protein kinases and function to regulate cell morphology (6, 27, 47). Homologues of these kinases are involved in hypha formation in *C. albicans* (8, 26, 28).

In this study, we took a genetic approach to define the role of myosin I in *C. albicans*. We found that myosin I is required for hypha but not pseudohypha formation and that the PAK phosphorylation site (serine 366) is critical for myosin I function during budding yeast and hyphal growth.

MATERIALS AND METHODS

DNA manipulations. The oligonucleotides used for cloning are listed in Table 1. The *CaMYO5* gene was amplified by PCR from genomic DNA prepared from *C. albicans* strain SC5314 by using the UO5 and UO6 oligonucleotides. The PCR products were digested with *Bam*HI and *Hin*dIII as well as with *Hin*dIII and *Xba*I. The 3.75- and 1.5-kb fragments were subcloned into pBluescript KS (Stratagene)to give pU14 and pU15, respectively. Several independent clones were verified by sequencing. The alignment of these sequences revealed the existence of two alleles for *CaMYO5* in SC5314, as expected for a diploid organism. The allele that was used for subsequent cloning was different from the sequence available in the Stanford genomic database for amino acids R354K, T585A, A596T, and I954V and for a short deletion, Δ1046–1051. The complete gene was reconstituted by subcloning a 3.75-kb *Bam*HI-*Hin*dIII fragment from pU14 and a 1.5-kb *Hin*dIII-*Xba*I fragment from pU15 into pKS and pVEC (35) digested with *Bam*HI and *Xba*I to give pU46A and pU67, respectively. These fragments were also subcloned into pRS316 and pRS426 digested with *Bam*HI and *Xba*I to give pU47 and pU48, respectively.

To construct the disruption cassette containing the *hisG::URA3::hisG* blaster (15), the 5′ noncoding region of *CaMYO5* was PCR amplified from genomic DNA by using UO9 and UO10, and the 3′ noncoding region was amplified with UO11 and UO6. These PCR products were digested with *Kpn*I and *Bam*HI and with *Bam*HI and *Xba*I, respectively, and subcloned together into pKS digested with *Kpn*I and *Xba*I (pU20). p5921 (15) was digested with *Pst*I and *Bam*HI, and the 4.0-kb fragment containing the *hisG::URA3::hisG* blaster was cloned into pU20 digested with *Bam*HI and *Pst*I. To construct the disruption cassette containing the *HIS1* gene, a 5′-flanking sequence was PCR amplified from genomic DNA by using UO36 and UO37. The 2-kb product was digested with *Kpn*I and *Bam*HI and subcloned into pU18 containing the 3′-flanking sequence of *CaMYO5* (pU72). Then, the *HIS1* gene was PCR amplified by using oligonucleotides CBF20 and CB20R (kind gifts from Catherine Bachewich), and the PCR product was digested with *Not*I and *Bam*HI and subcloned into pU72 digested first with *Bam*HI and then partially with *Not*I to generate pU74.

To construct *CaMYO5-GFP*, pU46A was digested with *Hin*dIII and *Xba*I, and

the 1.5-kb fragment containing the sequences of the *CaMYO5* tail domain was subcloned into pKS (pU15). A *Hin*dIII-*Pst*I site was created 5′ to the stop codon of *CaMYO5* in pU15 by using the reverse primer with UO26 and by using UO27 with UO6. The 1.5-kb PCR product was subcloned as a *Hin*dIII-*Xba*I fragment into pKS (pU50). A 700-base *Hin*dIII-*Pst*I fragment encoding green fluorescent protein (GFP) from pGFP26 (38) and a 1-kb *Kpn*I-*Hin*dIII partial fragment from pU50 were subcloned into pU50 digested with *Kpn*I and *Pst*I (pU88). Several clones were verified by sequencing. Finally, a 2.2-kb *Xba*I-*Hin*dIII partial fragment from pU88 and a 3.5-kb *Hin*dIII-*Bam*HI fragment from pU46A were subcloned together into pVEC digested with *Bam*HI and *Xba*I to generate pU93.

The S366A and S366D mutant alleles of *CaMYO5* were obtained by site-directed mutagenesis by using a Quick Change kit from Stratagene. First, the mutations were introduced into pU14 by PCR with *Pfu* polymerase and by using primer UO28 with primer UO29 (S366A mutation; pU55) and primer UO30 with primer UO31 (S366D mutation; pU56). These clones were sequenced to ensure that the S366A and S366D mutations were introduced while no other mutations had occurred. A 3.75-kb *Bam*HI-*Hin*dIII fragment from each of pU55 and pU56 and a 1.5-kb *Hin*dIII-*Xba*I fragment from pU15 were subcloned into pVEC digested with *Bam*HI and *Xba*I (pU77 and pU78, respectively). Similarly, the 3.75-kb *Bam*HI-*Hin*dIII fragments and a 2.2-kb *Hin*dIII-*Xba*I fragment from pU88 were subcloned into pVEC to create pU97 and pU98, which contain the S366A and S366D mutant alleles of *CaMYO5* in frame with the GFP sequence, respectively.

To express the S366A and S366D mutant alleles of *CaMYO5* under the control of the *PCK1* regulatable promoter, 4.75-kb fragments were PCR amplified from pU77 and pU78 by using UO19 and UO20. These fragments were digested with *Bgl*II and *Bam*HI and subcloned into pJA24 (*PCK1* promoter in p5921; a kind gift from J. Ash) digested with *Bgl*II (pU95 and pU96, respectively). Clones were kept in which the fragments were oriented such that the ATG of *CaMYO5* was immediately downstream of the *PCK1* promoter.

Transformations in *C. albicans* and *S. cerevisiae*. The strains used in this study are listed in Table 2. Transformation of *C. albicans* and *S. cerevisiae* strains was done by the lithium acetate method (21). To create a mutant in which both copies of the *CaMYO5* gene were deleted, the Ura⁻ strain CAI4 (15) and the Ura⁻ His⁻ strain RM1000 (39) were transformed with pU21 digested with *Kpn*I and *Sac*I. Genomic DNA was prepared from Ura⁺ transformants, digested with *Spe*I, and analyzed for the correct integration event by Southern blotting with a digoxigenin system (Boehringer Mannheim). Positive transformants derived from strain CAI4 were plated on medium containing 5-fluoroorotic acid (Diagnostics Chemicals Ltd., Charlottetown, Prince Edward Island, Canada), a drug which inhibits the growth of Ura⁺ strains. Ura⁻ strains thus obtained were analyzed similarly for the loop-out event that occurs by homologous recombination between the *hisG* direct repeats flanking the *URA3* gene. The *CaMYO5/Camyo5::hisG* strain was transformed with pU21 digested with *Kpn*I and *Sac*I. Ura⁺ transformants were analyzed similarly for the correct integration event resulting in the disruption of the second *CaMYO5* allele with the

TABLE 2. Strains

Strain	Genotype	Reference or source
C. albicans		
SC5314	*CaMYO5/CaMYO5 CaURA3/CaURA3*	15
CAI4	*ura3::1 imm434/ura3::1 imm434*	15
RM1000	CAI4 *Cahis1::hisG/Cahis1::hisG*	39
COU13	CAI4 *CaMYO5/Camyo5::hiG-URA3-hisG*	This study
COU42	CAI4 *Camyo5::hisG/Camyo5::hisG-URA3-hisG*	This study
COU46	CAI4 *Camyo5::hisG/Camyo5::hisG*	This study
COU73	CAI4 *Camyo5::hisG/Camyo5 (CaMYO5)*	This study
COU186	CAI4 *Camyo5::hisG/Camyo5 (CaMYO5-GFP)*	This study
COU190	CAI4 *Camyo5::hisG/Camyo5 (Camyo5^{S366A})*	This study
COU201	CAI4 *Camyo5::hisG/Camyo5 (Camyo5^{S366D})*	This study
COU232	CAI4 *Camyo5::hisG/Camyo5 (Camyo5^{S366D}-GFP)*	This study
COU243	CAI4 *Camyo5::hisG/Camyo5 (Camyo5^{S366A}-GFP)*	This study
CLJ4	CAI4 *Cacla4::hisG/Cacla4::hisG*	28
S. cerevisiae HA31-9c	*MAT**a** can1-100 ade2-1 his3-11 leu2-3, 112 ura3-1 trp1-1 myo3::HIS3 myo5::TRP1*	18

hisG::URA3::hisG blaster. A positive *Camyo5::hisG/Camyo5::hisG::URA3::hisG* transformant, called COU42, was analyzed for the correct loop-out event by plating on 5-fluoroorotic acid as described above. In parallel, positive transformants derived from the disruption of the first allele of *CaMYO5* in RM1000 were transformed with 5 μg of a PCR-amplified *Camyo5::CaHIS1* cassette by using UO6 and UO36. Transformants that were Ura$^+$ and His$^+$ were screened by Southern blot analysis for the disruption of the second allele with the *CaHIS1* marker as described above. Nineteen positive transformants were thus obtained that displayed phenotypes similar to that of COU42.

The *CaMYO5*, *CaMYO5^{S366A}*, *CaMYO5^{S366D}*, *CaMYO5-GFP*, *CaMYO5^{S366A}-GFP*, and *CaMYO5^{S366D}-GFP* alleles were integrated into the *Camyo5/Camyo5* Ura$^-$ mutant. First, pU67, pU77, pU78, pU93, pU97, and pU98 were linearized with *Bgl*II and transformed by the lithium acetate method into COU46 (COU42 Ura$^-$). The integration of each of these *CaMYO5* alleles at the *CaMYO5::hisG* locus was verified by Southern blot analysis. The overexpressed *CaMYO5^{S366A}* and *CaMYO5^{S366D}* alleles were integrated into the *Cacla4/Cacla4* Ura$^-$ mutant (CLJ4) (28). For this purpose, 10 μg each of pU95 and pU96 was linearized with *Xho*I and transformed by the lithium acetate method into CLJ4. The integration of these alleles at the *PCK1* locus was also verified by Southern blot analysis.

To determine functional complementation of the *CaMYO5* gene in the *S. cerevisiae myo3 myo5* mutant strain, pRS316/426, pVL62 (*MYO5* in pRS316; a kind gift from Cunle Wu), pU47, and pU48 were transformed into HA31-9c (18). Single colonies were streaked on 1% yeast extract–2% peptone–2% D-glucose (YPD) plates and grown at either 30 or 37°C for 3 days.

Phenotypic analyses. Media used for the hypha induction experiments were as follows: YPD supplemented with 10% heat-inactivated fetal bovine serum (FBS; Gibco BRL), 2% agar supplemented with 10% FBS, Spider medium (1% nutrient broth, 1% mannitol, 0.2% potassium phosphate [pH 7.2]), SLAHD medium (16), and Lee's medium (30).

Strains were grown in YPD overnight, and 30 μl of a 10^{-5} dilution was spread on one-sixth of a plate (agar-FBS, Spider, SLAHD, or Lee's medium). Plates were incubated for 4 days at 37°C. Colonies were visualized by using an inverted Nikon TMS microscope with a ×2 objective and a ×10 projection lens. Strains from the overnight cultures were also diluted to 1:20 in YPD supplemented with 10% fetal calf serum and were incubated for different times at 37°C. Cells were visualized by Nomarski optics by using an upright Leitz Aristoplan microscope with a ×40 objective or a ×100 immersion oil objective and a ×10 projection lens. For testing the phenotypes of the derived *cla4* deletion strains, these and wild-type strain SC5314 were grown overnight in YPD or YPCa (1% yeast extract–2% peptone–2% Casamino Acids). Cultures were diluted to 1:20 in YPD or YPCa, respectively, supplemented with 10% FBS and were incubated for 3 h at 37°C.

Doubling times for each strain were determined starting from three independent colonies grown overnight in YPD and diluted to an optical density at 600 nm (OD$_{600}$) of 0.1 at the beginning of the time course. The OD$_{600}$ values were determined every hour for up to 7 h.

Fluorescence. Overnight cultures in YPD of the various strains were diluted to 1:20 in either YPD or YPD with 10% FBS and grown for 3 h at 30 or 37°C, respectively. For GFP fluorescence, cells were washed once in phosphate-buffered saline (PBS) and mounted on slides for visualization with the appropriate filter by epifluorescence microscopy by using an upright Leitz Aristoplan micro-

scope with a ×100 immersion oil objective and a ×10 projection lens. For 4′,6′-diamino-2-phenylindole (DAPI; Sigma) and Calcofluor White (Sigma) staining, cells were fixed in 70% ethanol for 20 min and washed once with PBS. Cells were then stained for 5 to 10 min with either a 1:1,000 dilution of DAPI at 1 mg/ml or a 1:1,000 dilution of Calcofluor White at 1 mg/ml. Cells were washed extensively with PBS before visualization with the appropriate filter. For rhodamine-phalloidin (Molecular Probes, Eugene, Oreg.) staining, cells were fixed in medium with 3.7% formaldehyde (final concentration) for 30 min. After the cells were resuspended in 50 mM potassium phosphate buffer (pH 6.6) (PK buffer), they were fixed with 3.7% formaldehyde for 1 h. After one wash in PK buffer, cells were incubated for 30 min in PK buffer containing 0.1% Triton X-100. Cells were washed twice with PBS and incubated with a 1:10 dilution of rhodamine-phalloidin (200 U/ml) in PBS overnight at 4°C. After the supernatant was removed, cells were resuspended in PBS and visualized directly with the appropriate filter. DAPI staining was done at the last step with no further washing.

Video microscopy. Overnight cultures of COU73, COU186, COU201, COU232, and SC5314 were diluted to 1:1,600 in YPD supplemented with 10% FBS. Live video microscopy was done at 37°C by using a Leica DM-IRB inverted microscope equipped with a Ludl motorized stage, a temperature-controlled Δt culture dish system (Bioptechs), and a Sensys charge-coupled device camera. Pictures were taken with a ×40 objective and a ×10 projection lens every 15 min and in five different locations. Lengths of hyphae at different time points for more than 25 hyphae per strain were measured by using Openlab 3.1 software. The hyphal growth rate distribution for each strain was then determined. *t* tests were performed to determine the difference of means for COU73 versus COU201 and for COU186 versus COU232. The means were found to be significantly different in each set ($P < 10^{-6}$).

Protein extracts and Western blot analysis. Overnight cultures of COU186, COU232, COU243, and SC5314 grown in YPD were diluted to 1:100 in fresh YPD and grown to late exponential phase (OD$_{600}$, 2 to 3). Cells were centrifuged and frozen as a pellet at −80°C. Cells were subsequently lysed by vortexing with glass beads 10 times for 15 s each time at 4°C in lysis buffer (50 mM Tris-HCl [pH 7.5], 100 mM NaCl, 10 mM EDTA, 0.1% Triton X-100) containing protease inhibitors (10 mM Pefabloc, 50 μg of pepstatin A/ml, 50 μg of E64/ml, and 50 μg of aprotinin/ml) (Boehringer Mannheim). Lysates were cleared by centrifugation for 2 min at 10,000 × *g*. Protein extracts (50 μg) were loaded on a 6% acrylamide gel and separated by sodium dodecyl sulfate-polyacrylamide gel electrophoresis. Proteins were then transferred to a nitrocellulose membrane (Bio-Rad) for Western blot analysis with a 1:1,000 dilution of anti-GFP polyclonal antibody (a kind gift from B. Massie) followed by a 1:2,000 dilution of anti-rabbit horseradish peroxidase-conjugated immunoglobulin G (Santa Cruz Biotechnology). GFP fusion proteins were detected by enhanced chemiluminescence (Roche Diagnostics GmbH).

RESULTS

A single gene encodes myosin I in *C. albicans*. A search of the *C. albicans* sequence database (Stanford University) identified a single gene, *CaMYO5*, that encodes myosin I in *C.*
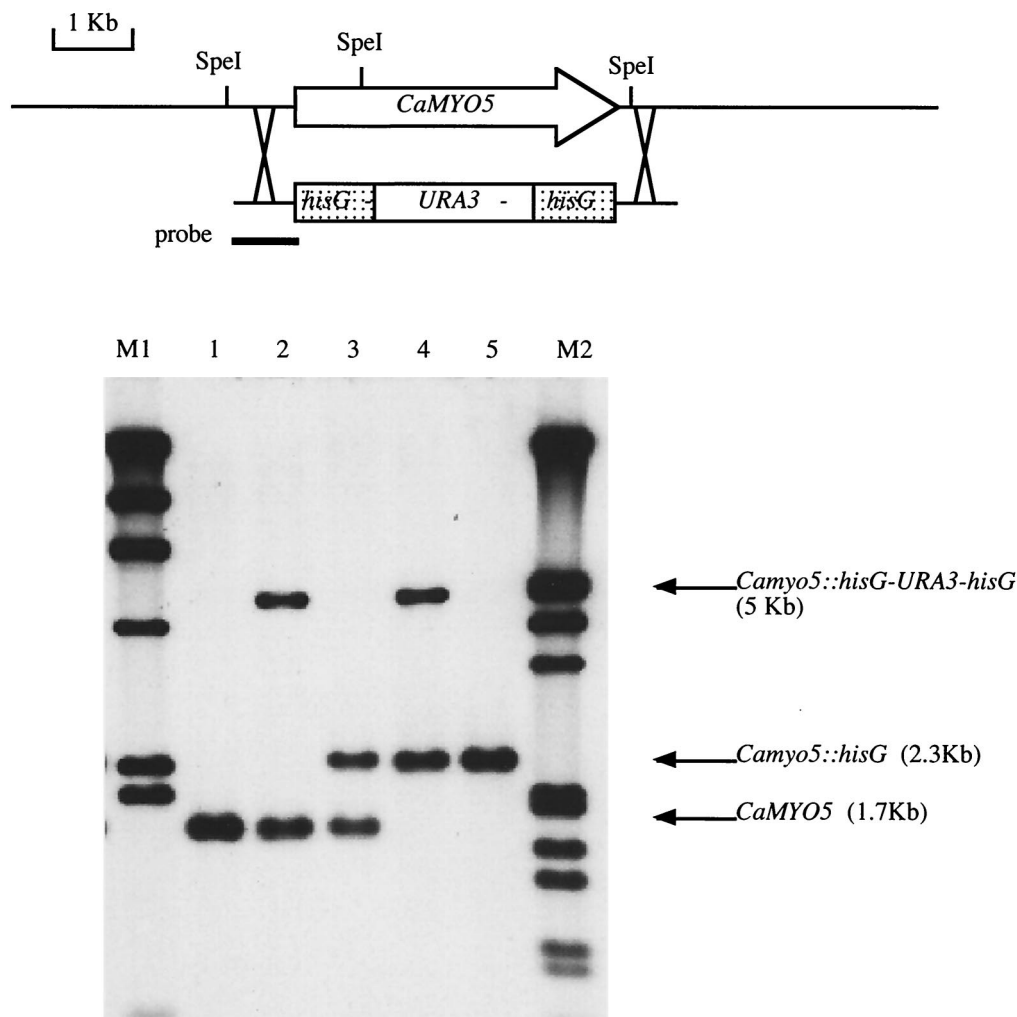
FIG. 1. Sequential disruption of both alleles of *CaMYO5*. Genomic DNA from strains was digested with *Spe*I and analyzed by Southern blotting with a probe encompassing the 5′ noncoding region of *CaMYO5* (thick line). Lanes: 1,CAI4 (wild type; Ura⁻); 2, *CaMYO5/ Camyo5::hisG-URA3-hisG*; 3, *CaMYO5/Camyo5::hisG*; 4, *Camyo5::hisG-URA3-hisG/Camyo5::hisG*; 5, *Camyo5::hisG/Camyo5::hisG*; M1, bands of 23, 9.4, 6.6, 4.4, 2.3, and 2.0 kb; M2, bands of 21, 5.1, 5.0, 4.3, 3.5, 2.0, 1.9, 1.6, 1.4, 0.9, and 0.8 kb.

albicans. In contrast, two such genes, *MYO3* and *MYO5*, are found in *S. cerevisiae* (18). The presence of a single myosin I-encoding gene was confirmed by low-stringency Southern blotting of *C. albicans* genomic DNA probed with a sequence corresponding to the SH3 domain of *CaMYO5* (data not shown). *CaMYO5* was amplified from genomic DNA prepared from wild-type strain SC5314 by PCR with specific oligonucleotides designed according to the sequence in the database. The PCR products were cloned, and four independent clones were sequenced to confirm their identities. The amino acid sequence was aligned with those of the Myo3 and Myo5 proteins of *S. cerevisiae*. On average, the amino acid sequence of CaMyo5 is 40% identical with those of Myo3 and Myo5. The highest conservation is found for residues in the N-terminal head domain involved in motor activity and including the TEDS-rule site (data not shown).

To determine if *CaMYO5* is a functional homologue of the *S. cerevisiae MYO3* and *MYO5* genes, the *C. albicans* gene was introduced into *S. cerevisiae* strain HA31-9c (18), which is

temperature sensitive due to deletion of the *MYO3* and *MYO5* genes. This strain could grow at the restrictive temperature when carrying *MYO5* on a centromeric plasmid (pVL62) but not when carrying the vector alone (pRS316) (data not shown). When this strain carried the *CaMYO5* gene on a multicopy plasmid, it could grow at the restrictive temperature, but it barely grew when carrying *CaMYO5* on a centromeric plasmid (data not shown). Thus, the overexpression of *CaMYO5* can complement the growth defect of *myo3 myo5* strains.

Myosin I is not essential for viability in *C. albicans*. To study the role of myosin I in *C. albicans*, we created a strain in which both copies of *CaMYO5* were deleted (Δ/Δ *Camyo5*). Figure 1 shows the sequential disruption of both alleles of *CaMYO5* in *C. albicans* (for details, see Materials and Methods). A single Δ/Δ *Camyo5* transformant was obtained starting from strain CAI4 (15), and 19 Δ/Δ *Camyo5* transformants were obtained starting from strain RM1000 (39). The latter strain is auxotrophic for histidine as well as uracil, enabling the disruption of each allele with a different marker (*CaHIS1* and *CaURA3*).

	Nomarski	Rhodamine-phalloidin	DAPI

SC5314

Camyo5/Camyo5

Camyo5/Camyo5
[*CaMYO5*]

Camyo5/Camyo5
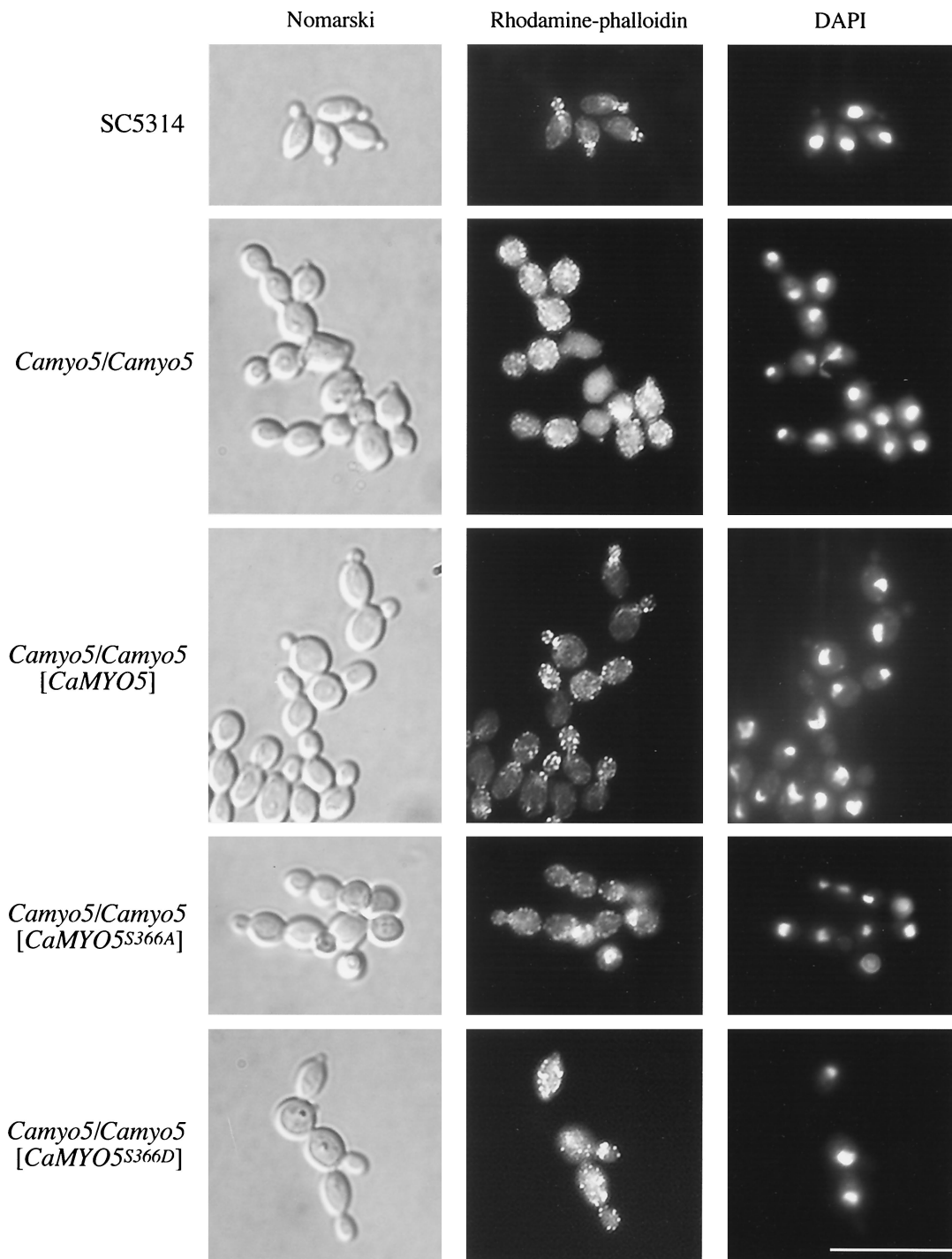[*CaMYO5*S366A]

Camyo5/Camyo5
[*CaMYO5*S366D]

FIG. 2. Cortical actin patch patterns in wild-type and mutant cells. Cells were fixed and stained with rhodamine-phalloidin. Nuclear DNA was stained with DAPI. Scale bar, 10 μm.

These 20 Δ/Δ *Camyo5* mutants displayed similar phenotypes, as described below. The ability to generate viable double-mutant strains indicates that the myosin I gene is not an essential gene in *C. albicans*.

Myosin I is required for the polarized distribution of cortical actin patches. We examined cells of the Δ/Δ *Camyo5* mutant and the wild-type strain (SC5314) microscopically for phe-

notypes that would indicate the role played by myosin I in budding yeast cells. Cells of the Δ/Δ *Camyo5* mutant viewed by Nomarski optics looked abnormally round, in some instances enlarged, and were clumped compared to wild-type cells (Fig. 2). To determine whether cortical actin patches were mislocalized in the Δ/Δ *Camyo5* mutant, we treated cells grown exponentially with rhodamine-phalloidin to stain filamentous actin.

TABLE 3. Cortical actin patch patterns in yeast cells[a]

Pattern	Appearance		% of cells of the following strain with the indicated pattern:			
	DAPI	RP	SC5314	Δ/Δ	Δ/Δ (CaMYO5)	Δ/Δ (CaMYO5^{S366D})
Polarized in bud			68.8	2.9	70.5	6.9
Loose			0	13.3	0	16.0
Depolarized			0	43.7	0	41.5
Polarized in bud; nuclear division			18.0	1.5	17.6	4.8
Depolarized; nuclear division			1.2	31.1	2.8	21.0
Bud neck; cytokinesis			8.1	0.7	7.7	0.5
Bud neck, loose; cytokinesis			1.9	6.6	0.7	7.4
Depolarized; G$_1$			1.9	0	1.4	1.6
Total no. of cells			161	135	142	188

[a] DAPI, nuclear staining; RP, rhodamine phalloidin, F-actin staining. Polarized in bud, cortical actin patches localize exclusively in bud; loose, cortical actin patches localize preferentially in bud but also in mother cell; depolarized, cortical actin patches localize equally in bud and mother cell; nuclear division, nuclei dividing; bud neck, cortical actin patches localize exclusively at neck; bud neck, loose, cortical actin patches localize at bud neck preferentially but also in daughter and mother cells; cytokinesis, nuclei have completed division, and mother and daughter cells are about the same size; G$_1$, no apparent budding. Scale bar, 1 μm.

Localization of cortical actin patches in budding cells of *S. cerevisiae* and *C. albicans* has been described extensively (4, 44). In summary, cortical actin patches localize to the growing bud tip, redistribute evenly in an isotropic growing bud, and finally localize at the mother bud neck after cytokinesis. In our experiments, cortical actin patches in 69% of wild-type cells were entirely localized to the buds during early bud emergence

and growth (Fig. 2 and Table 3). These patches remained in the buds of 18% of cells during and after nuclear division. These patches also were localized at the mother bud neck in 10% of cells. Strikingly, for the Δ/Δ *Camyo5* mutant, only 3% of cells retained cortical actin patches exclusively in the buds. In this mutant, cortical actin patches were localized evenly in both the mother cell and the buds for 44% of cells before
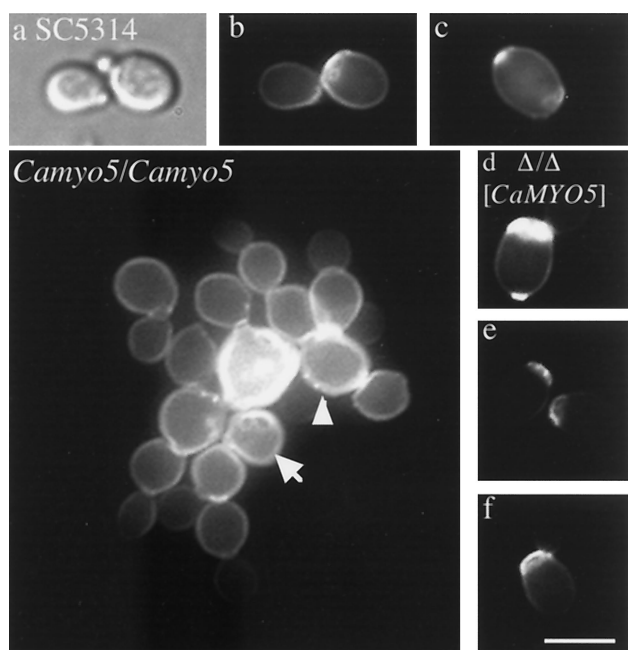
FIG. 3. Budding patterns of wild-type and *Camyo5/Camyo5* mutant strains. Cells were fixed and stained for chitin with Calcofluor White. (Panel a) Nomarski view. (Other panels) Calcofluor White staining. (a to c) SC5314. (d to f) reintegrant Δ/Δ (*Camyo5*) . Arrows indicate cells exhibiting random budding. In the large panel (*Camyo5/Camyo5*), the enlarged cell in the center shows abnormal chitin deposition in its cell wall. Scale bar, 4 μm.

nuclei had divided and in 31% of cells during nuclear division. Finally, in 7% of cells, the patches were localized at the mother bud neck while also localizing in daughter and mother cells. Overall, cortical actin patches are dramatically mislocalized in the Δ/Δ *Camyo5* mutant, suggesting that myosin I plays a role in the organization of the actin cytoskeleton.
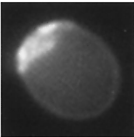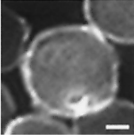
Myosin I plays a role in chitin deposition in the cell wall and in the budding pattern. To determine whether myosin I also plays a role in cell wall biogenesis in *C. albicans*, cells of the mutant and wild-type strains were labeled for chitin with Cal-

cofluor White. In the mutant, a small proportion of cells that were unusually enlarged and round showed aberrant chitin deposition in the cell wall (Fig. 3). These findings were not observed in the wild-type strain. At the same time, we found that nearly 20% of mutant cells exhibited a random budding pattern; the value for wild-type cells was 2% (Table 4). Mutations in actin or other cytoskeletal proteins lead to a high frequency of random budding patterns in diploid *S. cerevisiae* cells (11, 60). The higher incidence of random budding in the Δ/Δ *Camyo5* mutant than in the wild-type strain correlate with these data, suggesting that the actin-dependent mechanisms for bud site selection are similar in *C. albicans* and *S. cerevisiae*. In addition, *C. albicans* myosin I may be important for the regulation of cell wall biogenesis, based on the abnormal chitin deposition observed in the cell wall of the mutant.

Reintegration of wild-type myosin I in the null mutant leads to the recovery of wild-type characteristics. To determine whether the phenotypes of the mutant strain are due to the deletion of both copies of myosin I, the wild-type *CaMYO5* gene was reintegrated at one of the *CaMYO5* loci in a Ura⁻ strain (see Materials and Methods). Six transformants or "reintegrant" strains were thus obtained, and all exhibited normal cell shape. One reintegrant (COU73) was selected for more detailed analysis. This reintegrant exhibited normal cell shape (Fig. 2), cortical actin patch distribution (Fig. 2 and Table 3), and budding pattern (Fig. 3 and Table 4). Thus, the deletion of myosin I alone is responsible for the phenotypes of the Δ/Δ *Camyo5* strain.

Myosin I is required for the formation of hyphae on solid and in liquid media. We examined the ability of the Δ/Δ *Camyo5* mutant to form hyphae under different hypha-inducing conditions. The Δ/Δ *Camyo5* and wild-type (SC5314) strains were plated for single colonies on agar containing 10% FBS, Spider medium, SLAHD medium, or Lee's medium and were grown for 4 to 5 days at 37°C. The wild-type strain could form extensive hyphae on all media (Fig. 4A and data not shown). In contrast, the Δ/Δ *Camyo5* strain did not form hyphae on any medium (Fig. 4A and data not shown). Occasional extensions could be observed on parts of a Δ/Δ *Camyo5* colony grown on agar containing 10% FBS, but microscopic examina-

TABLE 4. Budding patterns[a]

Pattern	Appearance	% of cells of the following strain with the indicated pattern:				
		SC5314	*Camyo5/Camyo5*	Δ/Δ (*CaMYO5*)	Δ/Δ (*CaMYO5^{S366A}*)	Δ/Δ (*CaMYO5^{S366D}*)
Polar		97.7	80.6	98.6	83.2	90.2
Random		2.3	19.4	1.4	16.8	9.8
Total no. of cells		177	139	145	101	133

[a] Cells with more than two buds and/or bud scars were counted. Scale bar, 1 μm.
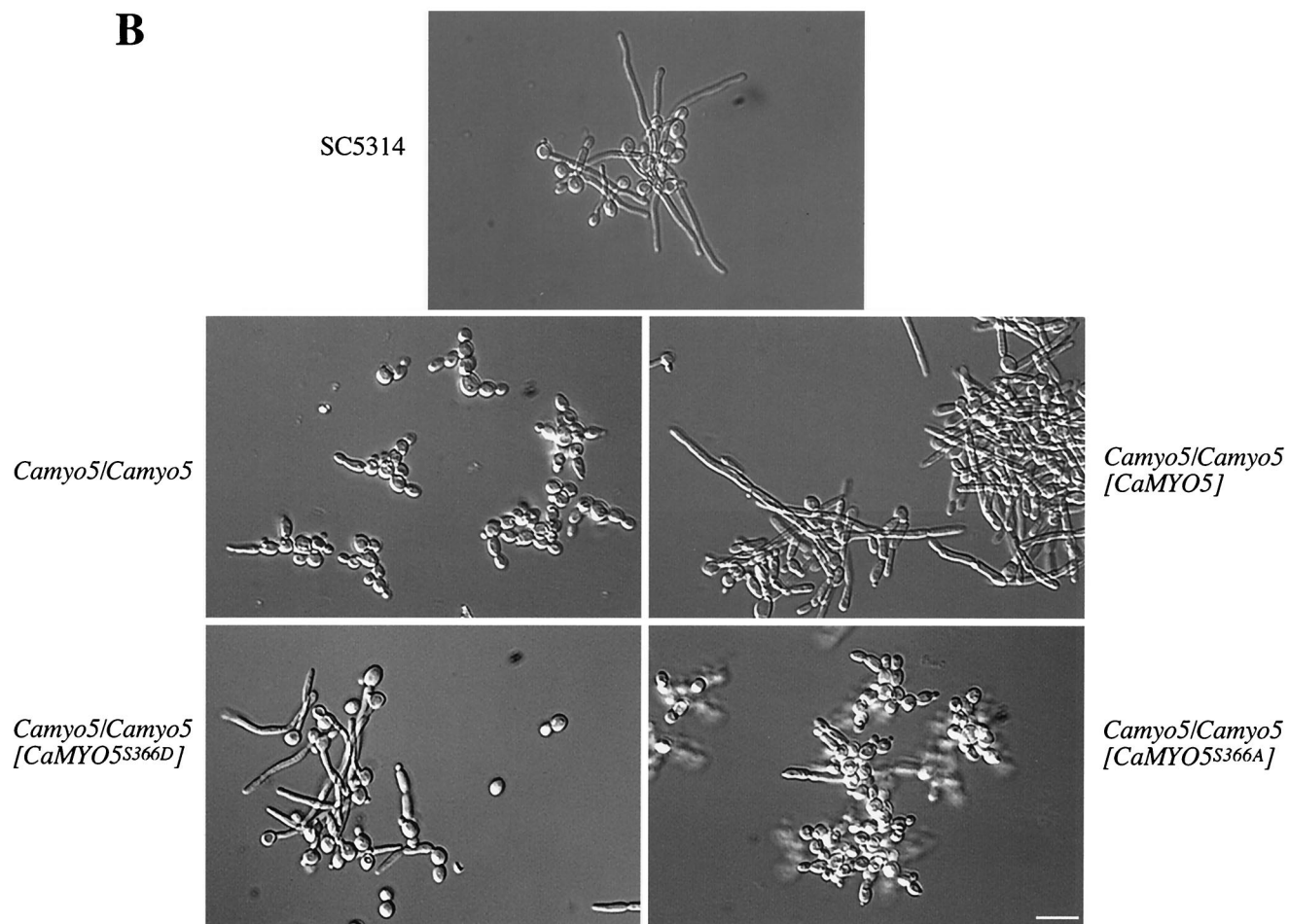
A
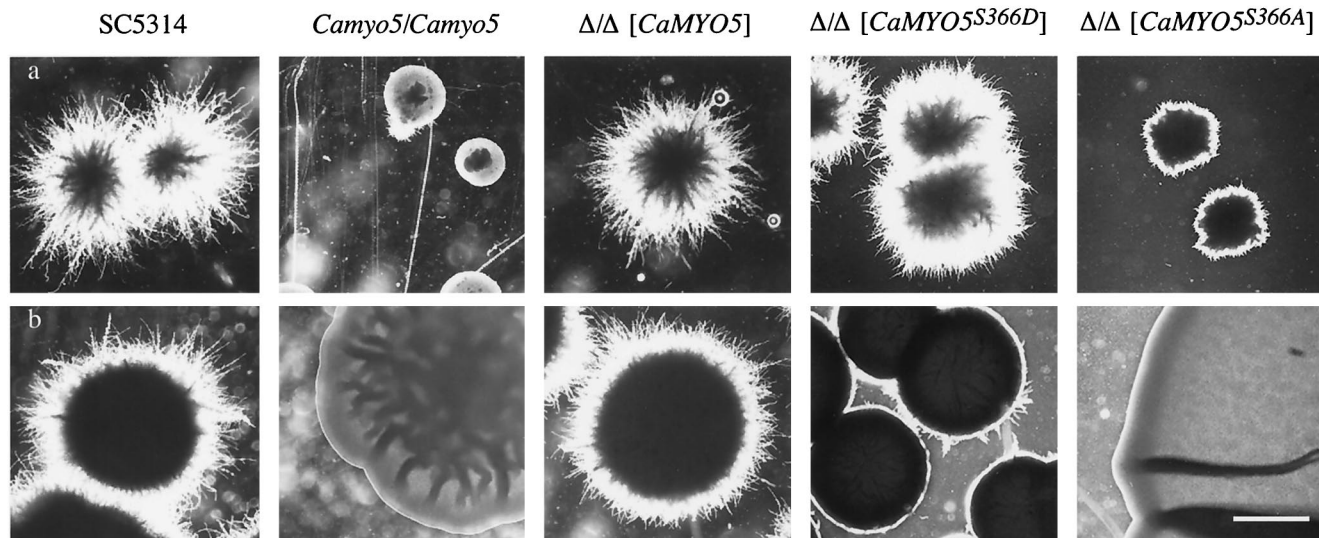
B

FIG. 4. Hypha formation in wild-type and mutant strains. (A) Hypha formation on solid media was determined by plating single colonies of each strain on 10% FBS (a) or Spider medium (b) plates. Plates were incubated for 4 days at 37°C. Scale bar, 1 mm. (B) Hypha formation in liquid YPD supplemented with 10% FBS was determined at 37°C after 2.5 h of incubation. Scale bar, 10 μm.

tion showed that these were formed by pseudohyphal cells (data not shown). To confirm that the deletion of myosin I alone was the cause of this nonhyphal phenotype, we tested the ability of the reintegrant strain to form hyphae under these conditions. This strain could form hyphae to the same extent as wild-type strain SC5314 (Fig. 4A and data not shown). These results indicate that myosin I is required for hypha formation on solid hypha-inducing media.

To determine cellular morphology under hypha-inducing conditions, cells were also incubated in liquid YPD medium containing 10% FBS or in Lee's medium at 37°C. After 2 to 3 h of incubation, cells of the wild-type strain formed germ tubes that extended into hyphae (Fig. 4B and data not shown). In contrast, cells of the Δ/Δ *Camyo5* strain occasionally formed germ tubes but were unable to form hyphae after more than 6 h of incubation in YPD medium containing serum or overnight incubation in Lee's medium, by which time the wild-type and reintegrant strains had formed extensive hyphae (data not shown). Pseudohyphal cells could be observed in the Δ/Δ *Camyo5* mutant instead (Fig. 4B). Because the Δ/Δ *Camyo5* strain could form pseudohyphae but not hyphae, it is possible that myosin I is required for maintaining polarized growth but not for initiating it.

Myosin I localizes to the bud and hyphal tips and partially colocalizes with cortical actin patches. To determine the localization of myosin I in *C. albicans*, we fused in frame the sequence encoding GFP (38) at the 3′ end of the *CaMYO5* open reading frame. We then introduced *CaMYO5-GFP* into the Ura⁻ Δ/Δ *Camyo5* strain, such that CaMyo5-GFP was the sole source of myosin I. Two independent transformants that were examined could form hyphae in the presence of serum. The CaMyo5-GFP protein in these transformants was detected by Western blot analysis as a band of 175 kDa (Fig. 5A). These results suggest that CaMyo5-GFP functions properly in the Δ/Δ *Camyo5* strain. Figure 5B shows the localization of CaMyo5-GFP in exponentially growing cells. CaMyo5-GFP clearly localized in patches at the tip of emerging buds. CaMyo5-GFP localization could also be observed at the mother bud neck after nuclear division was completed (Fig. 5B and data not shown). The localization of CaMyo5-GFP in hyphal cells was examined as well (Fig. 5C). CaMyo5-GFP localized in patches at the hyphal tip. The patch-like distribution of CaMyo5-GFP in budding and hyphal cells was similar to that of actin in cortical patches. To determine whether CaMyo5-GFP colocalizes with actin, we stained yeast cells and hyphal cells with rhodamine-phalloidin (Fig. 6). In most of the cells examined (108 of 120), there was either very good colocalization or partial colocalization of CaMyo5-GFP and cortical actin patches (two or more spots coinciding) either at the bud or hyphal tips or at the mother bud neck or septae (Fig. 6 and data not shown).

Serine 366 in myosin I is essential for normal growth and hypha formation. In several organisms, the ATPase activity of myosin I is increased by phosphorylation of a conserved serine residue in the head domain (10, 31, 56). In *S. cerevisiae*, this phosphorylation is catalyzed by activated Ste20 and Cla4 kinases (57). Ste20 and Cla4 are members of the PAK family of protein kinases which may be activated by Cdc42p and function to regulate cell morphology (26, 27). To determine whether the phosphorylation of myosin I by *C. albicans* PAK kinases is

important for hypha formation, we created mutant alleles of *CaMYO5* that code for alanine or aspartate instead of serine in the unique PAK phosphorylation site (serine 366). These alleles were reintroduced into the Δ/Δ *Camyo5* strain at the *Camyo5::hisG* loci (see Materials and Methods). Proper integration and expression of these alleles in several transformants were confirmed by Southern and Northern blot analyses, respectively (data not shown).

To determine whether *Camyo5*^{S366D} and *Camyo5*^{S366A} can rescue the phenotypes of the Δ/Δ *Camyo5* strain, we measured the growth rates of strains carrying these alleles and characterized their budding patterns. We found that the wild-type strain and the strain expressing *Camyo5*^{S366D} (COU201) divided every 55 min at 37°C in 2× YPD (Table 5). In contrast, the Δ/Δ *Camyo5* strain and the strain expressing *Camyo5*^{S366A} (COU190) divided every 69 min under the same growth conditions (Table 5). We also found that the S366A mutation increased random budding 10-fold, similar to the complete deletion of myosin I, while the S366D mutation increased random budding 5-fold (Table 4). Although there was no abnormal chitin deposition in cells expressing *Camyo5*^{S366D}, abnormal chitin staining could be observed in cells expressing *Camyo5*^{S366A} (data not shown). These results suggest that the phosphorylation of serine 366 is important for optimal growth and for cell wall biogenesis. Furthermore, phosphorylation of serine 366 may also be important, albeit to a lesser extent, for localization of the bud site. We also observed that the mutant expressing *Camyo5*^{S366D} did not form hyphal cells in YPD (Fig. 2), suggesting that other components of the actin cytoskeleton need to be activated to allow hypha formation under non-hypha-inducing conditions.

The mutant strains were plated for single colonies on agar containing 10% FBS and on Spider medium to determine their ability to form hyphae. All six transformants that expressed *Camyo5*^{S366D} formed fuzzy colonies similar to those of the wild-type and reintegrant strains (Fig. 4A). Under liquid hypha-inducing conditions, these cells were able to form hyphae as well. However, the numbers and rates of growth of the hyphae formed were lower than those of the wild-type strain (Fig. 4B and Table 6). The majority of seven transformants that expressed *Camyo5*^{S366A} formed fuzzy colonies with much shorter fringes than the wild-type and reintegrant strains on agar containing 10% FBS, but on the whole periphery of the colony, unlike the Δ/Δ *Camyo5* strain (Fig. 4A). On Spider medium, the colonies of the strain expressing *Camyo5*^{S366A} were consistently larger than those of the wild-type and Δ/Δ *Camyo5* strains. Microscopic examination revealed that colonies of this strain consisted of pseudohyphal cells (data not shown). In liquid YPD supplemented with 10% FBS or in Lee's medium, cells of the strain expressing *Camyo5*^{S366A} were unable to form hyphae but formed pseudohyphae to a greater extent than cells of the Δ/Δ *Camyo5* strain (Fig. 4B and data not shown). These results suggest that CaMyo5^{S366A} still retains some activity sufficient for more uniform pseudohyphal growth. Overall, the phosphorylation of serine 366 appears to be important for the proper function of CaMyo5 during hyphal growth.

To determine whether the TEDS-rule site serine 366 is important for the localization of myosin I, we tested the localization of CaMyo5^{S366A}-GFP and CaMyo5^{S366D}-GFP in normal
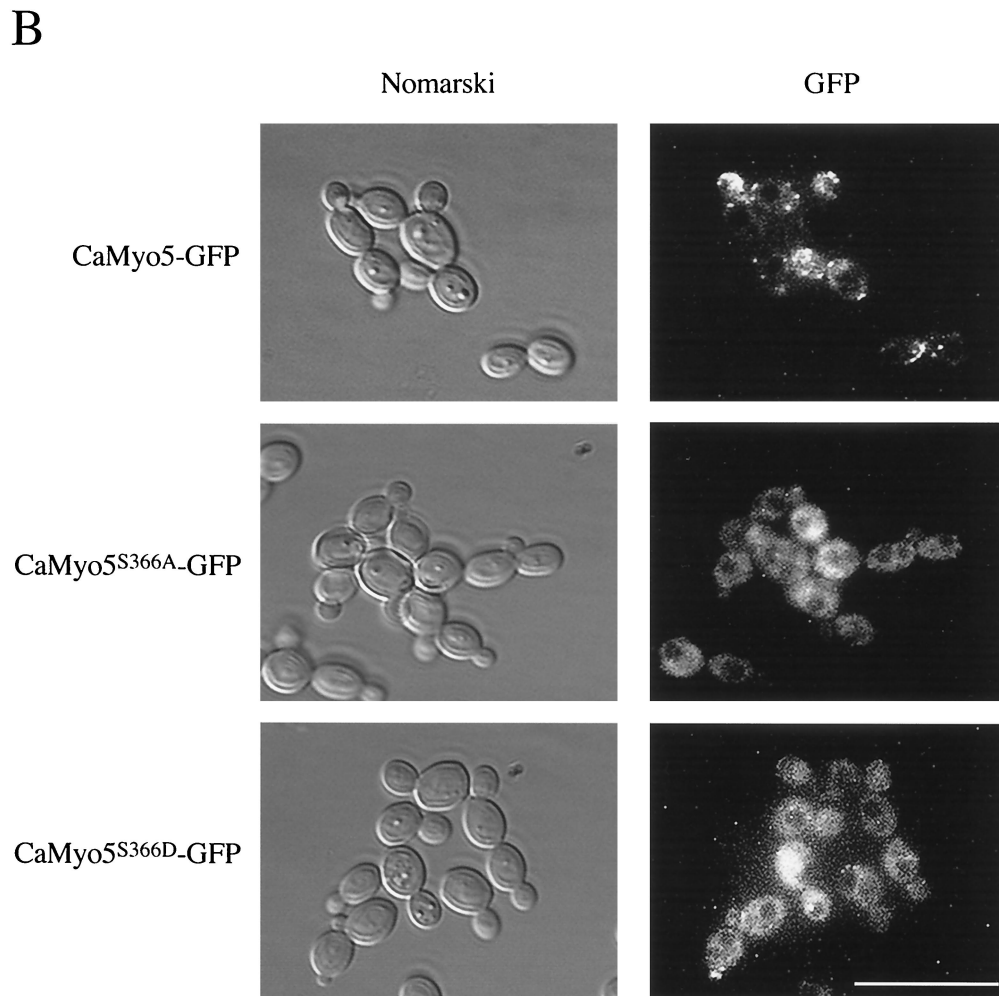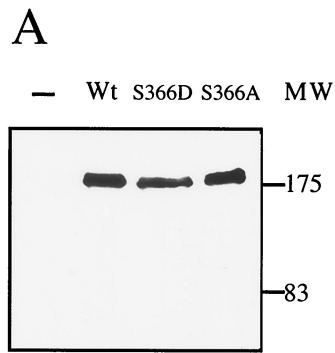
A

B

FIG. 5. Localization of wild-type and mutant CaMyo5-GFP. (A) Protein extracts (50 μg) prepared from cells expressing *CaMYO5-GFP* (Wt), *CaMYO5^S366D^-GFP* (S366D), or *CaMYO5^S366A^-GFP* (S366A) or from SC5314 (−) grown in YPD to late exponential phase were separated by sodium dodecyl sulfate-polyacrylamide gel electrophoresis on a 6% acrylamide gel. GFP fusion proteins were analyzed by Western blotting. Molecular weight markers (MW; in thousands) are indicated on the right. (B and C) Cells growing exponentially (B) or induced with 10% FBS at 37°C for 3 h (C) were visualized for GFP fluorescence. One of the wild-type hyphal cells moved during exposure, leading to a double exposure. Scale bars, 10 μm.

cells and elongated pseudohyphal or hyphal cells. These proteins were also detected by Western blot analysis as 175-kDa bands, and their levels were similar to the CaMyo5-GFP protein level (Fig. 5A). We found that the majority of CaMyo5^S366A^-GFP did not localize in cortical actin patches but localized in the cytoplasm (Fig. 5B and C). The majority of CaMyo5^S366D^-GFP did not localize to cortical actin patches either (Fig. 5B and C). Occasionally, some patches could be observed at the tips of buds, but these were not observed at hyphal tips. Mainly cytoplasmic staining and minor punctate

staining at the periphery could be observed in these hyphae. These results suggest that serine 366 is important for the proper localization of myosin I and, surprisingly, that the proper localization of myosin I at the hyphal tip is not required for hyphal growth.

Polarized distribution of cortical actin patches is dependent on serine 366. Because myosin I appeared mislocalized in the phosphorylation site mutants, we also determined the localization of cortical actin patches in these strains. Cortical actin patches were dramatically mislocalized to the mother cells
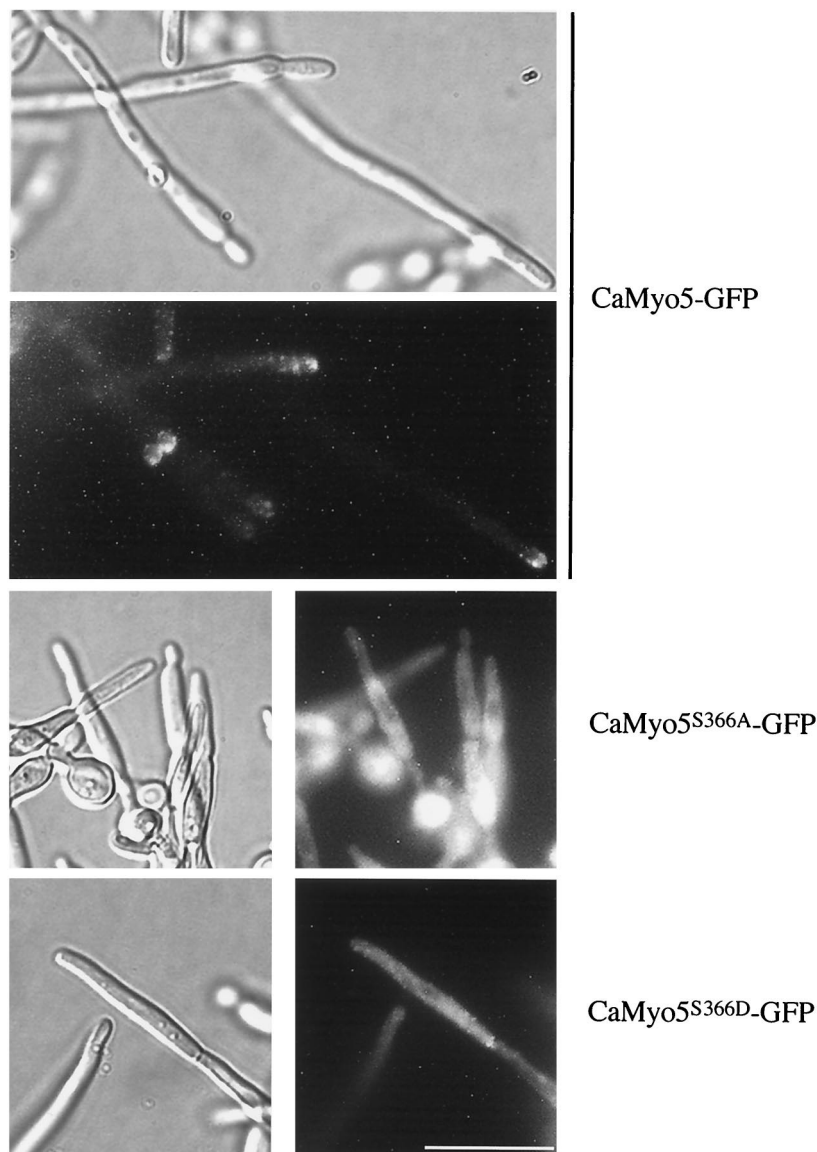
C

CaMyo5-GFP

CaMyo5^{S366A}-GFP

CaMyo5^{S366D}-GFP

FIG. 5—*Continued.*

(Fig. 2). The cortical actin patch distribution in cells expressing *Camyo5^{S366D}* was quantified more precisely (Table 3). Cortical actin patches were localized uniquely in the buds in only 7% of cells. They were also distributed in both the buds and the mother cell in 42% of cells prior to nuclear division and in 21% of cells after nuclear division. Finally, in 8% of cells, cortical actin patches were localized at the mother bud neck, while in most of these cells, they also were localized in the daughter and mother cells. Overall, cortical actin patches are mislocalized when serine 366 is mutated to alanine or aspartate, and the patterns of actin distribution are similar to those of the Δ/Δ *Camyo5* strain.

We also compared cortical actin patch distribution in hyphal cells expressing *Camyo5^{S366D}*, in pseudohyphal cells of both the Δ/Δ *Camyo5* strain and the strain expressing *Camyo5^{S366A}*, and in wild-type hyphal cells. In wild-type hyphal cells of *C. albicans*, cortical actin patches always localize at the tip throughout hyphal elongation (4). In contrast, cortical actin patch distribution in pseudohyphal cells of *S. cerevisiae* and *C. albicans* resembles that found in yeast cells (11) (data not shown). Surprisingly, we found that cortical actin patches localized evenly throughout pseudohyphal cells of the Δ/Δ *Camyo5* strain and strains expressing *Camyo5^{S366A}* and *Camyo5^{S366D}* (Fig. 7 and data not shown). In these mutants, very few tips of emerging pseudohyphal cells contained more cortical actin patches than the mother cells, in accordance with cortical actin patch patterns in yeast cells (data not shown). Surprisingly also, we found that cortical actin patches were
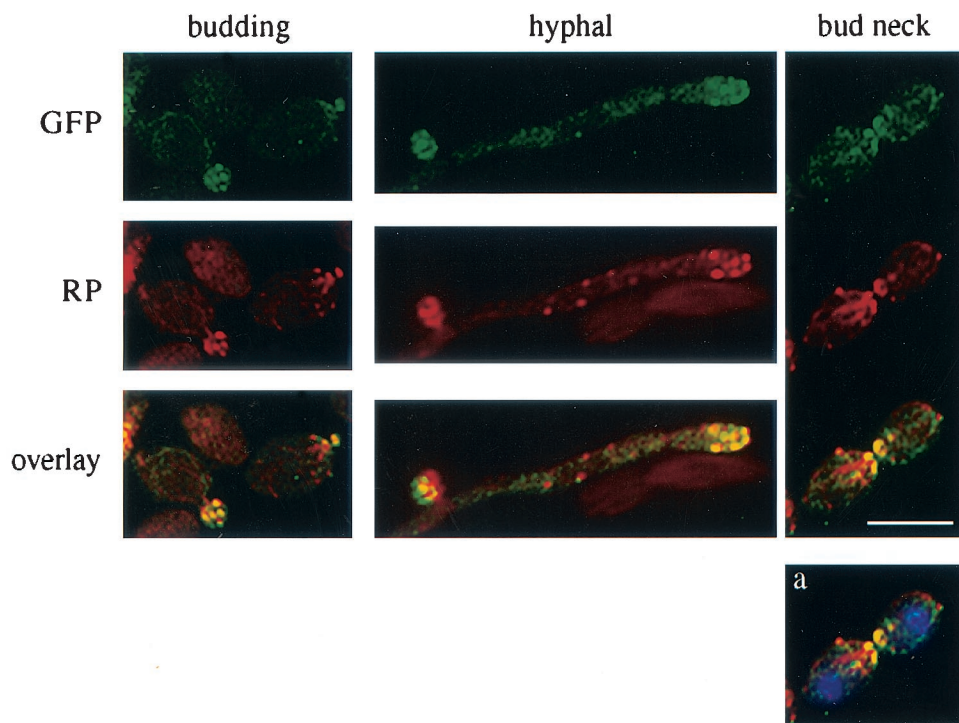
FIG. 6. Overlay of rhodamine-phalloidin and GFP signals. Budding and hyphal cells expressing CaMyo5-GFP were fixed and stained with rhodamine-phalloidin (RP) and DAPI. Pictures were taken with the appropriate filters to visualize CaMyo5-GFP (GFP), actin (RP), and nuclei (a). Overlays of the images were created with Adobe Photoshop, version 6.0. Scale bar, 4 μm.

localized throughout 66% of hyphal cells expressing *Camyo5^{S366D}* (Fig. 7 and Table 7). These patches localized at the tip of only 3% of hyphal cells in this mutant, while they localized at the tip of 75% of wild-type hyphal cells (Table 7). In addition, 14% of mutant hyphal cells showed an abnormal actin patch distribution rarely seen in wild-type cells. In these cells, cortical actin patches were found behind the hyphal tip (subapical). Overall, cortical actin patches were depolarized in the hyphae of the strain expressing *Camyo5^{S366D}*. These data indicate that cortical actin patch distribution is dependent on serine 366 in myosin I and suggest that a "tip-high" localization of cortical actin patches is not required for hyphal growth. Moreover, there is a strong correlation between myosin I localization and cortical actin patch distribution, because the strain expressing *CaMYO5^{S366D}-GFP* also exhibited a depolarized cortical actin patch distribution in 49% of hyphal cells; this value was 2% for the strain expressing *CaMYO5-GFP* (Table 7).

DISCUSSION

We used *C. albicans* as a model system to study polarized growth because this yeast is a human pathogen and can switch from the yeast form to the hyphal form under defined conditions. Moreover, through genetic screens and manipulations, several components have been identified that reveal aspects of the mechanisms involved in this transition (8, 55). The structural roles of the actin cytoskeleton and associated regulatory proteins are critical to hypha formation; mutations affecting these components have dramatic effects on polarized growth in different organisms (24, 41, 44). For instance, a homologue of a cortical actin patch component in *S. cerevisiae*, CaSla2p, is required for hypha formation in *C. albicans* (5).

Several observations reported here support a role for myosin I during polarized growth in *C. albicans*. First, cells with a deletion of for myosin I (Δ/Δ *Camyo5* strain) can form buds,

TABLE 5. Doubling times

Strain	Genotype	Doubling time (min, mean ± SD)[a]
SC5314	*CaMYO5/CaMYO5*	54.3 ± 1.5
COU42	*Camyo5/Camyo5*	68.2 ± 2.0
COU73	*Camyo5/Camyo5 (CaMYO5)*	54.8 ± 1.3
COU190	*Camyo5/Camyo5 (CaMYO5^{S366A})*	69.6 ± 2.0
COU201	*Camyo5/Camyo5 (CaMYO5^{S366D})*	57.7 ± 3.0

[a] Calculated from three independent colonies per strain.

TABLE 6. Hyphal growth rates[a]

Strain	Genotype	Growth rate (μm/h)	No. of hyphae
SC5314	Wild type	10.5	26
COU73	*Camyo5/Camyo5 (CaMYO5)*	11.7	29
COU186	*Camyo5/Camyo5 (CaMYO5-GFP)*	11.1	28
COU201	*Camyo5/Camyo5 (Camyo5^{S366D})*	7.7	29
COU232	*Camyo5/Camyo5 (CaMYO5^{S366D}-GFP)*	8.4	30

[a] The differences in the means for the hyphal growth rates for COU73 versus COU201 and for COU186 versus COU232 were significant at a *P* value of $<10^{-6}$.
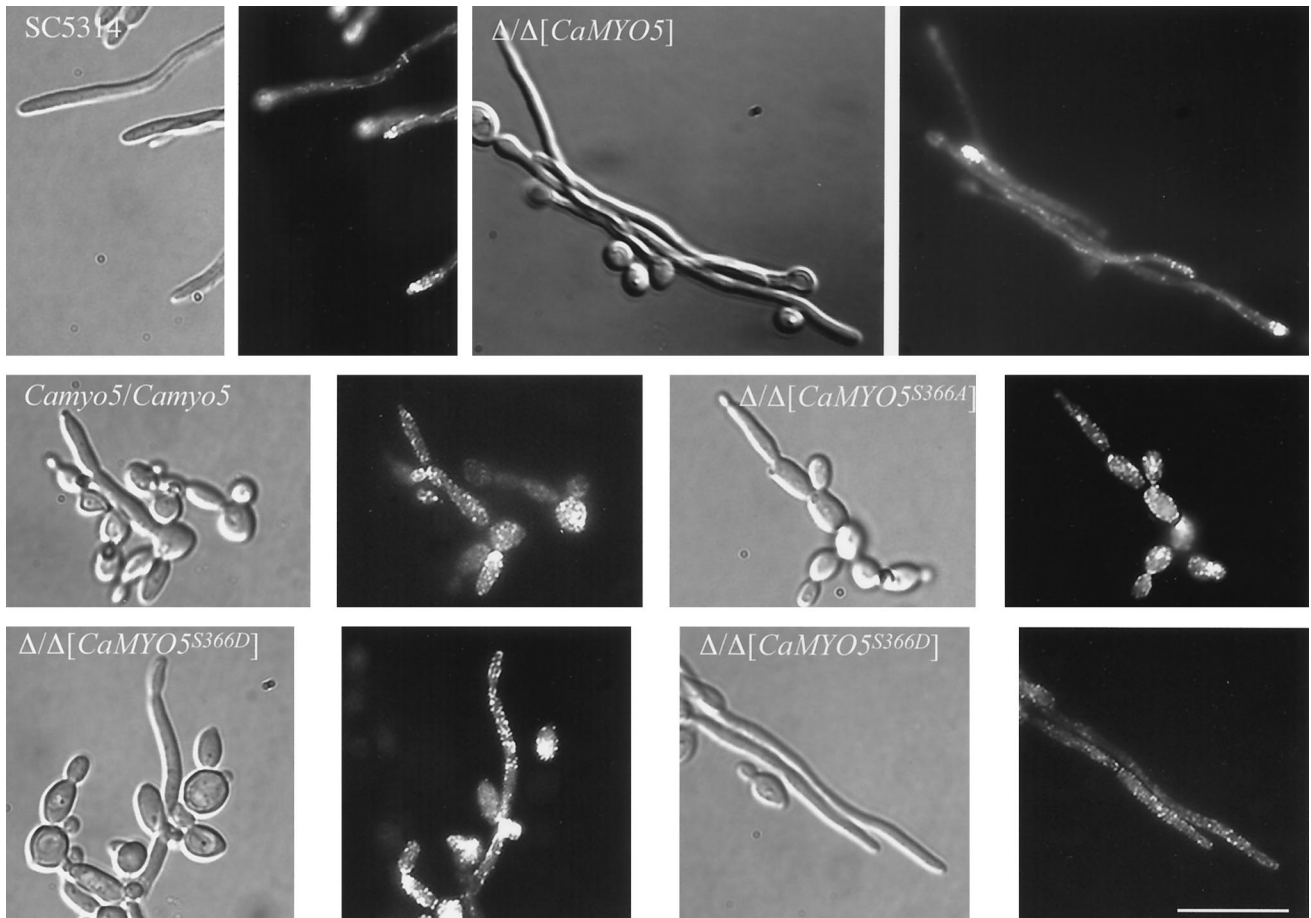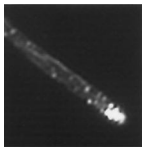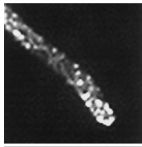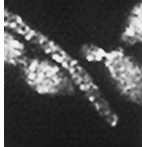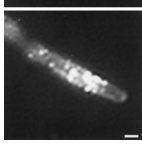
FIG. 7. Cortical actin patch patterns in wild-type and mutant hyphal and pseudohyphal cells. Hypha formation was induced with 10% FBS at 37°C for 3 h. Cells were then fixed and stained with rhodamine-phalloidin. The Nomarski image and the corresponding rhodamine-phalloidin image are shown for each strain. Scale bar, 10 μm.

but they are abnormally round and some are enlarged. Moreover, the Δ/Δ *Camyo5* strain fails to form true hyphae under hypha-inducing conditions. Second, CaMyo5-GFP in wild-type cells colocalizes with cortical actin patches at sites of polarized growth at the tips of buds and of hyphae. This localization pattern has been found for Myo5p and Myo3-GFP in *S. cerevisiae* and for MyoA-GFP in *Aspergillus* (3, 14, 59). Finally, while buds of wild-type *S. cerevisiae* and *C. albicans* strains grow apically initially and have localized actin patches at the tips (4, 44), the Δ/Δ *Camyo5* strain exhibits mislocalized cortical actin patches. In this mutant, cortical actin patches are largely dispersed throughout the bud as well as in the mother cell. This distribution could account for excessive isotropic growth resulting in the round and enlarged shape of the mutant cells. Overall, these results suggest that *C. albicans* myosin I is required for polarized cortical actin patch localization and are consistent with the role of myosin I in other organisms (3, 18, 32, 48).

We made several surprising observations relative to pseudohyphal and hyphal cells of *C. albicans*, suggesting that some differences in the mechanisms controlling polarized growth may exist between *C. albicans* and other organisms, including *S. cerevisiae*. First, we found that myosin I is not

essential and does not significantly impair growth in *C. albicans*. In *S. cerevisiae*, the two redundant genes encoding myosin I are either essential or important for growth, depending on the strain background (18, 57). Second, we found that myosin I is not required for pseudohypha formation in *C. albicans*, in contrast to the situation for *Aspergillus*, where deletion of *myoA* causes the complete inability to form polarized structures (36). Third, pseudohyphal cells of the Δ/Δ *Camyo5* mutant show mislocalized cortical actin patches, in contrast to *S. cerevisiae*, where pseudohypha formation requires a highly polarized actin cytoskeleton (11). This delocalized pattern of cortical actin patch distribution is also observed in the majority of hyphal cells of the mutant expressing *Camyo5^{S366D}*. This finding could explain the slow growth of these hyphae. Finally, we found that localization of myosin I to tips is not required for hypha formation, because hyphal cells were observed in the absence of polarized localization of myosin I in the strain expressing *Camyo5^{S366D}*. Thus, the formation of pseudohyphae and hyphae does not necessarily depend on polarized cortical actin patch and myosin I localization. However, treatment with cytochalasin A of cells of the wild-type, the Δ/Δ *Camyo5* strain, and the mutant expressing *Camyo5^{S366D}* inhibits germ tube

TABLE 7. Cortical actin patch patterns in hyphae[a]

Pattern	Appearance	% of hyphae of the following strain with the indicated pattern:				
		SC5314	Δ/Δ (CaMYO5)	Δ/Δ (CaMYO5-GFP)	Δ/Δ (CaMYO5^{S366D})	Δ/Δ (CaMYO5^{S366D}-GFP)
Polarized		74.3	77.7	87.0	3.1	7.8
Loose		20.0	18.4	12.2	18.8	30.0
Depolarized		4.3	3.9	1.7	65.6	48.9
Subapical		1.4	0	0	14.1	13.3
Total no. of hyphae		70	103	115	64	90

[a] Polarized, cortical actin patches localize exclusively at the hyphal tip; loose, cortical actin patches localize preferentially at the tip but also throughout the hyphae; depolarized, cortical actin patches localize throughout the hyphae; subapical, cortical actin patches localize beneath the tip. Scale bar, 1 μm.

formation (data not shown). These results suggest that some form of the actin cytoskeleton is essential for polarized growth.

To explain the formation of elongated cells despite the lack of cortical actin patch polarization, we suggest several possibilities. Perhaps only actin patches localizing at the hyphal tips of the mutant expressing *Camyo5*^{S366D} are functional. This would be the case if cortical actin patch components required for patch function preferentially localize at the hyphal tips of the mutant. Together with the small proportion of CaMyo5^{S366D} also localizing at the tips, this distribution may be sufficient to direct the growth of the hyphal form. On the other hand, the absence of myosin I and cortical actin patch components whose localization is dependent on myosin I may explain the hyphal defect of the Δ/Δ *Camyo5* mutant. In this regard, it would be interesting to determine the localization of key cortical actin patch components required for patch function in the various myosin I mutants. At least one cortical actin patch component, cofilin, is not found associated with actin patches in an *S. cerevisiae* myosin I mutant (48). Alternatively, other forms of actin that may specify polarized growth in *C. albicans*, such as actin cables, could be dependent on myosin I. The *S. cerevisae myo3 myo5* mutant shows defects in the organization of actin cables (18). It is therefore possible that the absence of hypha formation in the Δ/Δ *Camyo5* mutant can be explained by a defect in the organization of actin cables. Although the polarized localization of cortical actin patches is dependent on the presence of actin cables in *S. cerevisiae* and *S. pombe* (43, 45), the orientation of the cables may be restored and allow the formation of slowly growing hyphae in the mu-

tant expressing *Camyo5*^{S366D} in the absence of localized cortical actin patches. The importance of actin cables during polarized growth in *C. albicans* is presently uncertain, as we could not directly observe cables in the myosin I mutants, possibly because these were masked by cortical actin patches. Finally, it has been suggested that the transport of secretory vesicles occurs by dual microtubule- and actin-based systems (17). It is possible that when the actin-based system is impaired, vesicles are transported by a microtubule-based system.

Regulation of *C. albicans* myosin I function. We suggest that serine 366 of *C. albicans* myosin I is phosphorylated and that phosphorylation is required for the activity of myosin I, either by controlling the actin-dependent ATPase activity of the motor (56) or by controlling the interaction of myosin I with actin. That serine 366 is subject to phosphorylation is consistent with previous studies and is based on mutant phenotypes produced by mutations affecting this residue. Previous studies demonstrated that the phosphorylation of the TEDS-rule site in myosin I of different organisms is important for function. In one particular *S. cerevisiae* strain background (W303α), the phosphorylation of serine 357 in myosin I is essential (57). In *A. nidulans*, an S371E mutation introduces a residue that mimics a phosphorylated serine and leads to the accumulation of membranes in growing hyphae as a result of the hyperactivation of endocytosis. In contrast, an S371A mutation does not drastically affect this process (58). However, both of these mutations affect other aspects of cell growth and morphogenesis to the same extents, suggesting that the phosporylation of serine 371 per se does not regulate all functions of myosin I. In

Dictyostelium, serine 332 in myoB is essential for function, although it is not clear if phosphorylation plays a critical role (42). In *C. albicans*, an S366A mutation produces a slow-growth phenotype similar to that of the Δ/Δ *Camyo5* strain, while an S366D mutation does not impair growth in the yeast form. These data are analogous to the function of serine 361 in myosin I of fission yeast, where mutation to an alanine does not rescue the growth defect produced by a myosin I deficiency, but mutation to an aspartate does (53). Finally, a *C. albicans* myosin I mutant allele with the S366A mutation also does not allow the formation of hyphae, while the S366D mutation restores significant hyphal growth in response to hypha-inducing conditions. However, it appears that myosin I with aspartate 366 is less functional than wild-type myosin I. As discussed above, the S366D mutation results in the cytoplasmic localization of myosin I, as observed for myosin I fused to GFP. Moreover, the S366D mutation does not restore the polarized distribution of cortical actin patches in budding or hyphal cells. These results suggest that myosin I localization is required for the polarized distribution of cortical actin patches but is not a prerequisite for polarized growth.

To determine if the CaCla4 PAK kinase regulates the activity of myosin I by phosphorylating serine 366, we assessed whether the hyphal defect of the Δ/Δ *Cacla4* mutant can be overcome by overexpressing the phosphorylation mimic allele of myosin I, *CaMYO5^{S366D}*. We detected no major morphological differences between the Δ/Δ *Cacla4* mutants expressing wild-type levels of *CaMYO5* or overexpressing *CaMYO5^{S366D}* under hypha-inducing conditions (data not shown). Based on observations with *S. cerevisiae*, where the expression of Myo3^{S357D} could not overcome the lethality caused by the deletion of both *STE20* and *CLA4* (57), our results suggest that other targets of CaCla4 must be activated to bypass the hyphal defect of the Δ/Δ *Cacla4* mutant.

Mechanism of *C. albicans* myosin I function. Overall, it appears that the molecular mechanism by which myosin I acts in *C. albicans* is well conserved, as are its putative interacting partners, such as the Arp2/3 complex components (http://alces.med.umn.edu/Candida.html) (54). First, as in *S. cerevisiae* (3), in *C. albicans* myosin I appears not to be required for cortical actin patch formation but is required for the polarized localization of cortical actin patches in the bud and hyphal tips. Hence, *C. albicans* myosin I may regulate the activity of the Arp2/3 complex and target the polymerization of cortical actin patches to sites where it itself localizes. This interaction may be particularly critical for true hypha formation and may be regulated by phosphorylation of the TEDS-rule site by a homologue of the PAK kinases. We are currently investigating the role of serine 366 in the interaction of *C. albicans* myosin I with other proteins modulating actin polymerization.

ACKNOWLEDGMENTS

REFERENCES

1. **Adams, A. E., and J. R. Pringle.** 1984. Relationship of actin and tubulin distribution to bud growth in wild-type and morphogenetic-mutant *Saccharomyces cerevisiae*. J. Cell Biol. **98:**934–945.
2. **Akashi, T., T. Kanbe, and K. Tanaka.** 1994. The role of the cytoskeleton in the polarized growth of the germ tube in *Candida albicans*. Microbiology **140:**271–280.
3. **Anderson, B. L., I. Boldogh, M. Evangelista, C. Boone, L. A. Greene, and L. A. Pon.** 1998. The Src homology domain 3 (SH3) of a yeast type I myosin, Myo5p, binds to verprolin and is required for targeting to sites of actin polarization. J. Cell Biol. **141:**1357–1370.
4. **Anderson, J. M., and D. R. Soll.** 1986. Differences in actin localization during bud and hypha formation in the yeast *Candida albicans*. J. Gen. Microbiol. **132:**2035–2047.
5. **Asleson, C. M., E. S. Bensen, C. A. Gale, A. S. Melms, C. Kurischko, and J. Berman.** 2001. *Candida albicans INT1*-induced filamentation in *Saccharomyces cerevisiae* depends on Sla2p. Mol. Cell. Biol. **21:**1272–1284.
6. **Bagrodia, S., and R. A. Cerione.** 1999. Pak to the future. Trends Cell Biol. **9:**350–355.
7. **Bement, W. M., and M. S. Mooseker.** 1995. TEDS rule: a molecular rationale for differential regulation of myosins by phosphorylation of the heavy chain head. Cell Motil. Cytoskel. **31:**87–92.
8. **Brown, A. J., and N. A. Gow.** 1999. Regulatory networks controlling *Candida albicans* morphogenesis. Trends Microbiol. **7:**333–338.
9. **Brzeska, H., and E. D. Korn.** 1996. Regulation of class I and class II myosins by heavy chain phosphorylation. J. Biol. Chem. **271:**16983–16986.
10. **Brzeska, H., B. M. Martin, and E. D. Korn.** 1996. The catalytic domain of *Acanthamoeba* myosin I heavy chain kinase. I. Identification and characterization following tryptic cleavage of the native enzyme. J. Biol. Chem. **271:**27049–27055.
11. **Cali, B. M., T. C. Doyle, D. Botstein, and G. R. Fink.** 1998. Multiple functions for actin during filamentous growth of *Saccharomyces cerevisiae*. Mol. Biol. Cell **9:**1873–1889.
12. **Doberstein, S. K., I. C. Baines, G. Wiegand, E. D. Korn, and T. D. Pollard.** 1993. Inhibition of contractile vacuole function in vivo by antibodies against myosin-I. Nature **365:**841–843.
13. **Durrbach, A., K. Collins, P. Matsudaira, D. Louvard, and E. Coudrier.** 1996. Brush border myosin-I truncated in the motor domain impairs the distribution and the function of endocytic compartments in an hepatoma cell line. Proc. Natl. Acad. Sci. USA **93:**7053–7058.
14. **Evangelista, M., B. M. Klebl, A. H. Tong, B. A. Webb, T. Leeuw, E. Leberer, M. Whiteway, D. Y. Thomas, and C. Boone.** 2000. A role for myosin-I in actin assembly through interactions with Vrp1p, Bee1p, and the Arp2/3 complex. J. Cell Biol. **148:**353–362.
15. **Fonzi, W. A., and M. Y. Irwin.** 1993. Isogenic strain construction and gene mapping in *Candida albicans*. Genetics **134:**717–728.
16. **Gimeno, C. J., P. O. Ljungdahl, C. A. Styles, and G. R. Fink.** 1992. Unipolar cell divisions in the yeast *S. cerevisiae* lead to filamentous growth: regulation by starvation and *RAS*. Cell **68:**1077–1090.
17. **Goode, B. L., D. G. Drubin, and G. Barnes.** 2000. Functional cooperation between the microtubules and actin cytoskeletons. Curr. Opin. Cell Biol. **12:**63–71.
18. **Goodson, H. V., B. L. Anderson, H. M. Warrick, L. A. Pon, and J. A. Spudich.** 1996. Synthetic lethality screen identifies a novel yeast myosin I gene (*MYO5*): myosin I proteins are required for polarization of the actin cytoskeleton. J. Cell Biol. **133:**1277–1291.
19. **Hall, A., and C. D. Nobes.** 2000. Rho GTPases: molecular switches that control the organization and dynamics of the actin cytoskeleton. Philos. Trans. R. Soc. Lond. B Biol. Sci. **355:**965–970.
20. **Heath, I. B., G. Gupta, and S. Bai.** 2000. Plasma membrane-adjacent actin filaments, but not microtubules, are essential for both polarization and hyphal tip morphogenesis in *Saprolegnia ferax* and *Neurospora crassa*. Fungal Genet. Biol. **30:**45–62.
21. **Ito, H., Y. Fukuda, K. Murata, and A. Kimura.** 1983. Transformation of intact yeast cells treated with alkali cations. J. Bacteriol. **153:**163–168.
22. **Jung, G., K. Remmert, X. Wu, J. M. Volosky, and J. A. Hammer III.** 2001. The *Dictyostelium* CARMIL protein links capping protein and the Arp2/3 complex to type I myosins through their SH3 domains. J. Cell Biol. **153:**1479–1498.
23. **Karpova, T. S., S. L. Reck-Peterson, N. B. Elkind, M. S. Mooseker, P. J. Novick, and J. A. Cooper.** 2000. Role of actin and Myo2p in polarized secretion and growth of *Saccharomyces cerevisiae*. Mol. Biol. Cell **11:**1727–1737.
24. **Kost, B., R. J. Mathu, and N. H. Chua.** 1999. Cytoskeleton in plant development. Curr. Opin. Plant Biol. **2:**462–470.
25. **Kurischko, C., and R. K. Swoboda.** 2000. Cytoskeletal proteins and morphogenesis in *Candida albicans* and *Yarrowia lipolytica*, p. 173–184. *In* J. F. Ernst and A. Schmidt (ed.), Dimorphism in human pathogenic and apathogenic yeasts, vol. 5. S. Karger, Basel, Switzerland.

26. Leberer, E., D. Harcus, I. D. Broadbent, K. L. Clark, D. Dignard, K. Ziegelbauer, A. Schmidt, N. A. Gow, A. J. Brown, and D. Y. Thomas. 1996. Signal transduction through homologs of the Ste20p and Ste7p protein kinases can trigger hyphal formation in the pathogenic fungus *Candida albicans*. Proc. Natl. Acad. Sci. USA **93:**13217–13222.

27. Leberer, E., C. Wu, T. Leeuw, A. Fourest-Lieuvin, J. E. Segall, and D. Y. Thomas. 1997. Functional characterization of the Cdc42p binding domain of yeast Ste20p protein kinase. EMBO J. **16:**83–97.

28. Leberer, E., K. Ziegelbauer, A. Schmidt, D. Harcus, D. Dignard, J. Ash, L. Johnson, and D. Y. Thomas. 1997. Virulence and hyphal formation of *Candida albicans* require the Ste20p-like protein kinase CaCla4p. Curr. Biol. **7:**539–546.

29. Lechler, T., A. Shevchenko, and R. Li. 2000. Direct involvement of yeast type I myosins in Cdc42-dependent actin polymerization. J. Cell Biol. **148:**363–373.

30. Lee, K. L., H. R. Buckley, and C. C. Campbell. 1975. An amino acid liquid synthetic medium for the development of mycelial and yeast forms of *Candida albicans*. Sabouradia **13:**148–153.

31. Lee, S. F., T. T. Egelhoff, A. Mahasneh, and G. P. Côté. 1996. Cloning and characterization of a *Dictyostelium* myosin I heavy chain kinase activated by Cdc42 and Rac. J. Biol. Chem. **271:**27044–27048.

32. Lee, W. L., M. Bezanilla, and T. D. Pollard. 2000. Fission yeast myosin-I, Myo1p, stimulates actin assembly by Arp2/3 complex and shares functions with WASp. J. Cell Biol. **151:**789–800.

33. Machesky, L. M. 2000. The tails of two myosins. J. Cell Biol. **148:**219–221.

34. Machesky, L. M., and R. H. Insall. 1999. Signaling to actin dynamics. J. Cell Biol. **146:**267–272.

35. Magee, B. B., and P. T. Magee. 1997. WO-2, a stable aneuploid derivative of *Candida albicans* strain WO-1, can switch from white to opaque and form hyphae. Microbiology **143:**289–295.

36. McGoldrick, C. A., C. Gruver, and G. S. May. 1995. *myoA* of *Aspergillus nidulans* encodes an essential myosin I required for secretion and polarized growth. J. Cell Biol. **128:**577–587.

37. Mermall, V., P. L. Post, and M. S. Mooseker. 1998. Unconventional myosins in cell movement, membrane traffic, and signal transduction. Science **279:**527–533.

38. Morschhauser, J., S. Michel, and J. Hacker. 1998. Expression of a chromosomally integrated, single-copy *GFP* gene in *Candida albicans*, and its use as a reporter of gene regulation. Mol. Gen. Genet. **257:**412–420.

39. Negredo, A., L. Monteoliva, C. Gil, J. Pla, and C. Nombela. 1997. Cloning, analysis and one-step disruption of the *ARG5,6* gene of *Candida albicans*. Microbiology **143:**297–302.

40. Neuhaus, E. M., and T. Soldati. 2000. A myosin I is involved in membrane recycling from early endosomes. J. Cell Biol. **150:**1013–1026.

41. Noegel, A. A., and M. Schleicher. 2000. The actin cytoskeleton of *Dictyostelium*: a story told by mutants. J. Cell Sci. **113:**759–766.

42. Novak, K. D., and M. A. Titus. 1998. The myosin I SH3 domain and TEDS rule phosphorylation site are required for in vivo function. Mol. Biol. Cell **9:**75–88.

43. Pelham, R. J. J., and F. Chang. 2001. Role of actin polymerization and actin cables in actin-patch movement in *Schizosaccharomyces pombe*. Nat. Cell Biol. **3:**235–244.

44. Pruyne, D., and A. Bretscher. 2000. Polarization of cell growth in yeast. II. The role of the cortical actin cytoskeleton. J. Cell Sci. **113:**571–585.

45. Pruyne, D. W., D. H. Schott, and A. Bretscher. 1998. Tropomyosin-containing actin cables direct the Myo2p-dependent polarized delivery of secretory vesicles in budding yeast. J. Cell Biol. **143:**1931–1945.

46. Raposo, G., M. N. Cordonnier, D. Tenza, B. Menichi, A. Durrbach, D. Louvard, and E. Coudrier. 1999. Association of myosin I alpha with endosomes and lysosomes in mammalian cells. Mol. Biol. Cell **10:**1477–1494.

47. Sells, M. A., and J. Chernoff. 1997. Emerging from the PAK: the p21-activated protein kinase family. Trends Cell Biol. **7:**162–167.

48. Smith, M. G., S. R. Swamy, and L. A. Pon. 2001. The life cycle of actin patches in mating yeast. J. Cell Sci. **114:**1505–1513.

49. Soldati, T., H. Geissler, and E. C. Schwarz. 1999. How many is enough? Exploring the myosin repertoire in the model eukaryote *Dictyostelium discoideum*. Cell Biochem. Biophys. **30:**389–411.

50. Temesvari, L. A., J. M. Bush, M. D. Peterson, K. D. Novak, M. A. Titus, and J. A. Cardelli. 1996. Examination of the endosomal and lysosomal pathways in *Dictyostelium discoideum* myosin I mutants. J. Cell Sci. **109:**663–673.

51. Torralba, S., M. Raudaskoski, and A. Pedegrosa. 1998. Effects of methyl benzimidazole-2-yl carbamate on microtubule and actin cytoskeleton in *Aspergillus nidulans*. Protoplasma **202:**54–64.

52. Torralba, S., M. Raudaskoski, A. Pedegrosa, and F. Laborda. 1998. Effect of cytochalasin A on apical growth, actin cytoskeleton organization and enzyme secretion in *Aspergillus nidulans*. Microbiology **144:**45–53.

53. Toya, M., F. Motegi, K. Nakano, I. Mabuchi, and M. Yamamoto. 2001. Identification and functional analysis of the gene for type I myosin in fission yeast. Genes Cells **6:**187–199.

54. Tzung, K. W., R. M. Williams, S. Scherer, N. Federspiel, T. Jones, N. Hansen, V. Bivolarevic, L. Huizar, C. Komp, R. Surzycki, R. Tamse, R. W. Davis, and N. Agabian. 2001. Genomic evidence for a complete sexual cycle in *Candida albicans*. Proc. Natl. Acad. Sci. USA **98:**3249–3253.

55. Whiteway, M. 2000. Transcriptional control of cell type and morphogenesis in *Candida albicans*. Curr. Opin. Microbiol. **3:**582–588.

56. Wu, C., S. F. Lee, E. Furmaniak-Kazmierczak, G. P. Côté, D. Y. Thomas, and E. Leberer. 1996. Activation of myosin-I by members of the Ste20p protein kinase family. J. Biol. Chem. **271:**31787–31790.

57. Wu, C., V. Lytvyn, D. Y. Thomas, and E. Leberer. 1997. The phosphorylation site for Ste20p-like protein kinases is essential for the function of myosin-I in yeast. J. Biol. Chem. **272:**30623–30626.

58. Yamashita, R. A., and G. S. May. 1998. Constitutive activation of endocytosis by mutation of *myoA*, the myosin I gene of *Aspergillus nidulans*. J. Biol. Chem. **273:**14644–14648.

59. Yamashita, R. A., N. Osherov, and G. S. May. 2000. Localization of wild type and mutant class I myosin proteins in *Aspergillus nidulans* using GFP-fusion proteins. Cell Motil. Cytoskel. **45:**163–172.

60. Yang, S., K. R. Ayscough, and D. G. Drubin. 1997. A role for the actin cytoskeleton of *Saccharomyces cerevisiae* in bipolar bud-site selection. J. Cell Biol. **136:**111–123.

61. Yokoyama, K., H. Kaji, K. Nishimura, and M. Miyaji. 1990. The role of microfilaments and microtubules in apical growth and dimorphism of *Candida albicans*. J. Gen. Microbiol. **136:**1067–1075.